
Ant Colony Sampling with GFlowNets for Combinatorial Optimization

Minsu Kim^{1,5*} Sanghyeok Choi^{1*} Hyeonah Kim¹
Jiwoo Son^{2,6} Jinkyoo Park^{1,2} Yoshua Bengio^{3,4}

¹ KAIST ² Omelet ³ Mila – Québec AI Institute ⁴ Université de Montréal

Abstract

This paper introduces the Generative Flow Ant Colony Sampler (GFACS), a neural-guided probabilistic search algorithm for solving combinatorial optimization (CO). GFACS integrates generative flow networks (GFlowNets), an emerging amortized inference method, with ant colony optimization (ACO), a promising probabilistic search algorithm. Specifically, we use GFlowNets to learn a constructive policy in combinatorial spaces for enhancing ACO by providing an informed prior distribution over decision variables conditioned on input graph instances. Furthermore, we introduce a novel off-policy training algorithm for scaling conditional GFlowNets into large-scale combinatorial spaces by leveraging local search and shared energy normalization. Our experimental results demonstrate that GFACS outperforms baseline ACO algorithms in seven CO tasks and is competitive with problem-specific heuristics for vehicle routing problems.

1 Introduction

Combinatorial optimization (CO) is a crucial domain involving high-impact applications, including vehicle routing, hardware design optimization, and biological sequence design. Ant colony optimization (ACO) [14, 68] is a general-purpose meta-heuristic algorithm designed to address these tasks. ACO employs a constructive solution generation scheme that sequentially adds elements to a partial solution, known for its flexibility across CO tasks. This approach involves collecting experiences from multiple agents (*ants*) to iteratively update a distribution (*pheromone update*) based on a prior distribution known as the *heuristic matrix*. The major benefits of ACO include: (1) its robustness against local optima, enabled by the algorithm’s stochastic nature, which dynamically balances exploration and exploitation, preventing premature convergence [14]; and (2) its flexible solution generation scheme, which allows it to effectively solve a wide range of combinatorial optimization tasks [79].

The main challenge with ACO lies in designing effective *prior distributions* (i.e., the heuristic matrix) for their probability models. Inadequate priors can lead to time-consuming pheromone update iterations. Recent advancements, known as DeepACO [79], address this by using policy gradient reinforcement learning (RL) [76, 71] to pretrain the priors conditioned on given problem instances. RL trains these networks to guide highly rewarded regions, allowing generalization to new problems and enhanced performance.

* Equal contribution.

⁵ Work performed while the author was at the Mila – Québec AI Institute

⁶ Work performed while the author was at the KAIST

Correspondence to: Minsu Kim (min-su@kaist.ac.kr)

Motivated by DeepACO, we propose a deep learning-based prior distribution design. However, this paper tackles challenges related to the design of prior distribution through deep amortized inference rather than the policy gradient RL method. This is motivated by the following three primary limitations in DeepACO’s use of policy gradient RL. First (●), the on-policy nature of DeepACO restricts the flexible use of a behavior policy, potentially undermining performance by limiting effective exploration of vast combinatorial spaces. Second (●), the reward maximizing form of RL in DeepACO struggles to capture the diverse solutions necessary in CO, even though having a variety of good candidates could significantly enhance the likelihood of finding a global optimum after local searches. Last (●), the inherent symmetry in combinatorial solutions—where different paths can lead to identical outcomes—presents a significant challenge not adequately addressed in DeepACO.

Contribution. This paper introduces a novel ACO algorithm, the Generative Flow Ant Colony Sampler (GFACS), which addresses the limitations of DeepACO by integrating the emerging amortized inference method of GFlowNets [4, 5]. Our twofold contribution can be summarized as follows. (1) We introduce a new viewpoint to ACO using amortized inference instead of policy gradient RL. (2) Additionally, we present a novel GFlowNet training algorithm for large scale combinatorial tasks, applicable to a range of further uses over ACO.

ACO as off-policy amortized inference with GFlowNets. There are three reasons that GFlowNets can improve over the existing DeepACO algorithm. First (●), the off-policy training property of GFlowNets allows for the utilization of samples drawn from any behavior policy, including powerful heuristic search algorithms commonly used in CO problems. Secondly (●), unlike maximum reward-seeking algorithms (e.g., RL training in DeepACO), GFlowNets are sampling algorithms that are well-suited for modeling the multimodal nature of certain distributions. Lastly (●), GFlowNets model solutions as a generative process on a directed acyclic graph (DAG), which can represent multiple trajectories that share identical states. This approach allows for accurate probabilistic modeling by considering the symmetry of combinatorial solutions [5].

Scaling conditional GFlowNets into large-scale combinatorial space. GFlowNets often struggle with limited scalability due to challenging exploration problems [58, 39], credit assignment issues [59, 26], and unstable training when inferring conditional distributions [82]. In combinatorial optimization, both limitations must be addressed because we deal with (1) large-scale combinatorial spaces and (2) conditional inference on problem instances. This study introduces a new off-policy training method for GFlowNets in large combinatorial spaces by effectively leveraging local search operators. It also proposes a novel training method to address instability in training conditional GFlowNets by properly normalizing conditional reward values with sample mean.

In comparative experiments, our GFACS exhibits significant superiority over the current DeepACO and classical ACO algorithms for various representative CO tasks – vehicle routing problems, scheduling problems, and a grouping problem. Moreover, GFACS outperforms or shows similar performance to competitive unsupervised learning-based vehicle routing solvers, which are designed to solve traveling salesman problems (TSP) and capacitated vehicle routing problems (CVRP) in the context of large-scale instances, such as $N = 500, 1000$. Lastly, we compared our approach with previous GFlowNet methods for solving combinatorial optimization problems [82, 84] in vehicle routing tasks, which are known to pose challenges for credit assignment due to their locally undecomposable properties, as highlighted by Ahn et al. [1].

2 Related works

2.1 Ant colony optimization

Ant Colony Optimization (ACO) is a meta-heuristic inspired by ant behavior in finding optimal paths. Traditional ACO algorithms, such as Ant System (AS) [14] and MAX-MIN AS [68], rely on specific heuristics for success. To reduce the reliance on heuristic design, Ye et al. [79] introduce a neural-guided ACO, called DeepACO, utilizing graph representation learning and reinforcement learning to replace manual heuristics with automatically acquired knowledge.

2.2 Neural combinatorial optimization

Neural combinatorial optimization [3] is a deep learning-based method to train an instance-conditional policy using supervised learning [75, 20, 70] or unsupervised learning [30, 41, 43, 54].

Usually, supervised learning methods are beneficial when the target problem has an accurate but time-consuming expert solver. The oracle-labeled data is collected from the oracle solvers, and deep neural networks amortize the search process, converting an expensive run-time optimization into an also expensive but one-time cost of training the neural net, allowing for scalability and faster run-time inferences than the expert solver. On the other hand, unsupervised learning proceeds through self-guided trial and error, using the COP objective as a training signal. This makes it applicable even if encountering less-studied problems where powerful expert solvers are unavailable [3, 1]. Our method can be categorized as an unsupervised learning method, which does not need expert labels. See [Appendix F](#) for a more comprehensive survey.

2.3 GFlowNets and combinatorial optimization

GFlowNets are designed for sampling combinatorial objects proportionally to a given reward function [4]. Theoretical studies have connected GFlowNets with variational inference [53] and maximum entropy reinforcement learning [56, 13]. Recent algorithmic advancements in GFlowNets have focused on developing new training objectives [52, 51, 85], enhancing credit assignment [59, 26], and improving exploration strategies [58, 63, 59, 39, 38].

GFlowNets have also found successful applications in some combinatorial optimization problems (COPs) [82, 84]. Zhang et al. [84] effectively address the symmetric nature of graph constraint optimization, demonstrating remarkable performance in tasks such as finding maximum independent sets. Despite their success, there are limitations in expanding to other combinatorial tasks due to their reliance on local credits for the learning objective proposed by Pan et al. [59]. Conversely, Zhang et al. [82] address proxy-based scheduling problems by developing a problem-specific neural architecture and introducing novel training methods for general-purpose conditional GFlowNets. One of their significant contributions is the proposal of a loss function based on the sample variance of the log partition function, known as VarGrad, which enhances the training process and performance.

3 Preliminary

3.1 Traveling salesman problem

The traveling salesman problem (TSP) is a fundamental combinatorial optimization problem, which serves as a building block for more complex CO problems like the capacitated vehicle routing problem (CVRP) and orienteering problem (OP). In light of this and for simplicity, this paper presents formulations using the two-dimensional Euclidean TSP as an illustrative example.

A TSP instance is defined on a (fully connected) graph $\mathcal{G} = \{\mathcal{V}, \mathcal{D}\}$, where \mathcal{V} and \mathcal{D} are a node set and edge set, respectively. Each node $i \in \mathcal{V}$ has two-dimensional coordinates $v_i \in [0, 1]^2$ as a feature, and each edge $(i, j) \in \mathcal{D}$ has a feature $d_{i,j}$ which is the distance between node i and j , i.e., $d_{i,j} = \|v_i - v_j\|_2$. A solution to TSP, $x(\mathcal{G})$ corresponds to a Hamiltonian cycle for a given problem instance \mathcal{G} , which can be represented as a permutation of nodes $\pi = (\pi_1, \dots, \pi_N)$. The tour length is computed as $\mathcal{E}(x(\mathcal{G})) = d_{\pi_N, \pi_1} + \sum_{t=1}^{N-1} d_{\pi_t, \pi_{t+1}}$. The optimization objective for TSP is to find $x(\mathcal{G})$ that minimizes $\mathcal{E}(x(\mathcal{G}))$.

3.2 Ant colony optimization

Ant colony optimization is a meta-heuristic to refine the solution sampling probability by an iterative procedure of solution construction and pheromone update. Given a problem instance \mathcal{G} , a corresponding heuristic matrix $\eta(\mathcal{G}) \in \mathbb{R}^{N \times N}$ and a pheromone trails $\rho \in \mathbb{R}^{N \times N}$, a solution is constructed by auto-regressively sampling edges from the probability distribution:

$$P(\pi_{t+1} = j | \pi_t = i; \rho, \eta(\mathcal{G})) \propto \begin{cases} \rho_{i,j} \eta_{i,j}(\mathcal{G}) & \text{if } j \notin \pi_{1:t} \\ 0 & \text{otherwise,} \end{cases} \quad (1)$$

where $\rho_{i,j}$ and $\eta_{i,j}(\mathcal{G})$ are the pheromone weight and heuristic weight for edge $d_{i,j}$, respectively.

At each iteration, K artificial ants independently sample solutions $\{\pi^k\}_{k=1}^K$ by following [Equation \(1\)](#). The pheromone trails ρ are then adjusted using the solution set and corresponding costs, thereby updating the solution construction probability. The pheromone update rules vary depending on the ACO algorithm used. For example, in Ant System (AS) [14], all K solutions contribute to

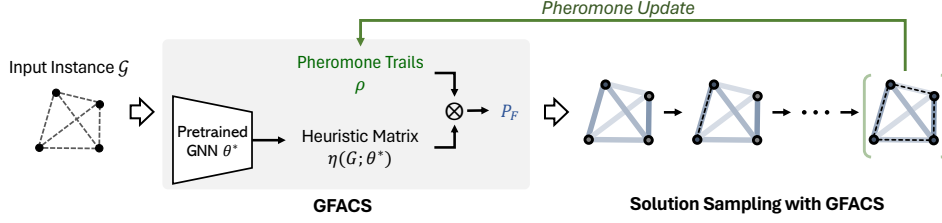


Figure 1: Solution sampling process of GFACS. The GNN, pretrained with a GFlowNet loss, serves as an expert heuristic to pick the next action to construct a solution, such as a tour in the TSP.

the pheromone update:

$$\rho_{i,j} \leftarrow (1 - \gamma)\rho_{i,j} + \sum_{k=1}^K \Delta_{i,j}^k, \quad (2)$$

where γ is the decaying coefficient (or evaporation rate) and $\Delta_{i,j}^k$ is the amount of pheromone laid by the k -th ant on the edge (i, j) . Here, $\Delta_{i,j}^k$ is proportional to the inverse of tour length if (i, j) is included in π^k , and zero otherwise.

$$\Delta_{i,j}^k = \begin{cases} C/f(\pi^k) & \text{if } (i, j) \in \pi^k \\ 0 & \text{otherwise} \end{cases} \quad (3)$$

where C is a constant. The smaller the cost $f(\pi^k)$, the more pheromone is laid on the edges of π^k .

Note that the heuristic matrix $\eta(\mathcal{G}) \in \mathbb{R}^{N \times N}$ is not updated during the search process; it only serves as a prior. ACO aligns the search process more closely with the most efficacious paths discovered; see Dorigo et al. [15] for details. In DeepACO [79], the learned graph neural network (GNN), parameterized by θ , is utilized to construct the heuristic matrix $\eta(\mathcal{G}, \theta)$ for a given problem instance \mathcal{G} , thereby providing a good prior for guiding probabilistic solution search process of ACO.

3.3 Generative flow networks

Generative Flow Networks, or GFlowNets [4, 5] provide an effective training framework for learning a policy that samples compositional objects denoted as $x \in \mathcal{X}$ towards the objective of generating x with probability proportional to a given non-negative reward function $R(x)$. GFlowNets follow a constructive generative process, using discrete *actions* to iteratively modify a *state* which represents a partially constructed object. All the ways to construct these objects can be described by a directed acyclic graph (DAG), $\mathcal{H} = (\mathcal{S}, \mathcal{A})$, where \mathcal{S} is a finite set of all possible states, and \mathcal{A} is a subset of $\mathcal{S} \times \mathcal{S}$, representing directed edges. Within this framework, we define the *children* of state $s \in \mathcal{S}$ as the set of states connected by edges whose head is s , and the *parents* of state s as the set of states connected by edges whose tail is s .

We define a *complete trajectory* $\tau = (s_0 \rightarrow \dots \rightarrow s_N) \in \mathcal{T}$ from the initial state s_0 to terminal state s_n . We denote $\tau_{\rightarrow x}$ when the terminal state s_n is finalized to the corresponding object $x \in \mathcal{X}$. We define the *forward policy* to model the forward transition probability $P_F(s'|s)$ from s to its child s' . Similarly, we also consider the *backward policy* $P_B(s|s')$ for the backward transition $s' \rightarrow s$, where s is a parent of s' . We can use the *forward policy* to compute in a forward way the probability of a trajectory: $P_F(\tau; \theta) = \prod_{t=1}^n P_F(s_t | s_{t-1}; \theta)$.

Similarly, we can use the *backward policy* to compute in a backward way the probability of trajectory ending at a given object $x = s_n$: $P_B(\tau_{\rightarrow x} | x; \theta) = \prod_{t=1}^n P_B(s_{t-1} | s_t; \theta)$.

Trajectory balance [52]. Trajectory balance is the most widely used training objective for GFlowNets. When the trajectory balance objective is minimized, we achieve that the probability of sampling x with the forward policy is $P_F^\top(x) \propto R(x)$, as desired, where $P_F^\top(x) = \sum_{\tau_{\rightarrow x} \in \mathcal{T}} P_F(\tau)$. The trajectory balance loss \mathcal{L}_{TB} works by training three models, a learnable scalar Z_θ for the partition function, a forward policy $P_F(\tau; \theta)$, and a backward policy $P_B(\tau_{\rightarrow x} | x; \theta)$ to minimize the following objective:

$$\mathcal{L}_{TB}(\tau; \theta) = \left(\log \frac{Z_\theta P_F(\tau; \theta)}{R(x) P_B(\tau_{\rightarrow x} | x; \theta)} \right)^2. \quad (4)$$

4 Generative flow ant colony sampler (GFACS)

In this section, we provide the inference procedure for the Generative Flow Ant Colony Sampler (GFACS). GFACS is a sampling algorithm that enhances Ant Colony Optimization (ACO) by integrating it with GFlowNets. The central concept is to use GFlowNets to generate an appropriate instance-conditioned prior (edge) distribution (heuristic matrix), which more effectively guides the probabilistic search procedure of ACO.

4.1 MDP formulation

The solution construction procedure by GFlowNets can be modeled as a Markov decision process (MDP). We illustrate this procedure using the Traveling Salesman Problem (TSP) as an example. This formulation can be easily adapted to general combinatorial optimization problem with minor modifications.

State s : The initial state s_0 is an empty set. The state s_t at $0 < t < n$ is a partial combinatorial solution of presented with previous actions: $\{a_0, \dots, a_{t-1}\}$ and s_n is completed solution.

Action a : The action a_t is a selection of a node to visit at time t among un-visited nodes: $a_t \in \{1, \dots, N\} \setminus \{a_0, \dots, a_{t-1}\}$. If all nodes are visited, a deterministic terminating action is applied, which maps a final state s_N into a solution, $x(\mathcal{G})$.

Reward $R(x(\mathcal{G}); \beta)$: The reward is defined as the unnormalized Boltzmann distribution of the solution $x(\mathcal{G})$ with energy $\mathcal{E}(x(\mathcal{G}))$. Specifically, the reward is given by $R(x(\mathcal{G}); \beta) = e^{-\beta \mathcal{E}(x(\mathcal{G}))}$. Here, $\mathcal{E}(x(\mathcal{G}))$ represents the energy of the solution $x(\mathcal{G})$, which corresponds to metrics such as the tour length in the TSP.

The coefficient β , known as the inverse temperature, is a hyperparameter.

4.2 Policy configuration

We parameterize the forward policy P_F using a graph neural network (GNN) with parameter θ that maps an input graph instance \mathcal{G} to the output edge matrix $\eta(\mathcal{G}; \theta)$, following Ye et al. [79]. Then, the forward policy when $t < N$ is expressed as follows:

$$P_F(s_{t+1}|s_t; \eta(\mathcal{G}; \theta), \rho) \propto \begin{cases} \rho_{a_{t-1}, a_t} \eta_{a_{t-1}, a_t}(\mathcal{G}; \theta) & \text{if } a_t \notin s_t \\ 0 & \text{otherwise} \end{cases} \quad (5)$$

Note that ρ and $\eta(\mathcal{G}; \theta)$ denote the pheromone trails and learned heuristic matrix in ACO. Subsequently, we can define a trajectory from the initial state to a terminal solution, with $\tau = (s_0, \dots, s_N, x(\mathcal{G}))$, and the forward probability of that trajectory,

$$P_F(\tau; \eta(\mathcal{G}; \theta), \rho) = \prod_{t=0}^{N-1} P_F(s_{t+1}|s_t; \eta(\mathcal{G}; \theta), \rho). \quad (6)$$

Note that the forward probability for the transition from s_N to $x(\mathcal{G})$ is omitted as it follows a deterministic rule.

For the backward policy, we set $P_B = \frac{1}{2N}$, emulating the maximum entropy GFlowNets [83] to make uniform exploration over symmetric trajectories which terminate into identical solution. Here, P_B represents a uniform distribution across all $2N$ feasible trajectories leading to a solution $x(\mathcal{G})$. This is particularly pertinent in the context of the TSP involving N cities, where $2N$ permutations culminate in the same Hamiltonian cycle $x(\mathcal{G})$. The count of symmetric trajectories depends on the task’s characteristics. For an exhaustive discussion on solution symmetry across various COPs, please refer to [Appendix E](#).

4.3 Solution sampling with GFACS

In the sampling process, we assume the existence of the learned GNN parameterized with θ^* ; see [Section 5](#) for details of the training procedure.

The learned GNN provides the heuristic matrix $\eta(\mathcal{G}; \theta^*)$ for ACO algorithm. Thus, the remaining process is to update pheromone parameter ρ with solutions sampled by $P_F(\tau; \eta(\mathcal{G}; \theta^*), \rho)$ during the solution searching process. As the $\eta(\mathcal{G}; \theta^*)$ is trained with GFlowNets to sample diverse high-rewarded (i.e., low energy) samples, P_F generates good candidates for updating ρ . The overall process is illustrated in Figure 1.

5 Off-policy training of GFACS

This section introduces how to train GFACS, especially the GNN component parameterized with θ , in the GFlowNet framework. GFACS is trained via iterations of the off-policy experience collection (Step A) and training (Step B).

5.1 Step A: Off-policy experience collection with local search and energy reshaping

In this step, we collect experiences on given graph instances. The experiences in step A will be used for training GFACS in step B. For every iteration, we first sample M problem instances from a random sampler $P(\mathcal{G})$, i.e., $\mathcal{G}_1, \dots, \mathcal{G}_M \sim P(\mathcal{G})$. Details of instance sampling are described in Appendix B. For each problem instance \mathcal{G}_m , we collect K solutions by following Eq. 6 as $\mathcal{B}_{\text{explore}} = \{(\mathcal{G}_m, \tau_{\rightarrow x_{m,k}}^{m,k}, \mathcal{E}(x_{m,k}))\}_{m=1, \dots, M, k=1, \dots, K}$.

To exploit high-reward regions in the large-scale combinatorial space, we also collect K exploitation samples for each \mathcal{G}_m using a local search operator (LS), such as 2-opt for TSP, as a powerful behavioral policy. The local search operator directly refines a given solution into a locally optimized one, i.e., $x' \leftarrow LS(x)$. We then use the backward policy P_B to sample a trajectory $\tau_{\rightarrow x'}$ for each x' , obtaining a batch of “exploitation experiences,” $\mathcal{B}_{\text{exploit}} = \{(\mathcal{G}_m, \tau_{\rightarrow x_{m,k}'}^{m,k}, \mathcal{E}(x_{m,k}'))\}_{m=1, \dots, M, k=1, \dots, K}$. Please note that we also suggest a general-purpose local search operator that partially destroys a solution and then repairs for problems that lack domain-specific local search methods. Please refer to Appendix C for details about the destroy-and-repair local search.

While the concept of using local search for exploitation has been explored in recent GFlowNet works [39], our distinct approach involves utilizing the local search (LS) operation to facilitate *hindsight observation*—a forward-looking insight derived from extending the search beyond the current state. We focus on evaluating samples that were initially overlooked due to their high energy (i.e., low reward) but can be transformed to exhibit low energy (i.e., high reward) following the local search.

To achieve this, we modify the energy (in a way we call *energy reshaping*) for the exploration around x in $\mathcal{B}_{\text{explore}}$ by using the energy of the refined solution $x' = LS(x)$ as follows:

$$\mathcal{E}_{\text{reshaped}}(x) = \alpha \mathcal{E}(x') + (1 - \alpha) \mathcal{E}(x). \quad (7)$$

5.2 Step B: Training with collected experiences with shared energy normalization

Given the collected experience batches $\mathcal{B}_{\text{explore}}$ and $\mathcal{B}_{\text{exploit}}$, we aim to minimize the following loss function:

$$\mathcal{L}(\theta) = \mathcal{L}(\theta; \mathcal{B}_{\text{explore}}) + \mathcal{L}(\theta; \mathcal{B}_{\text{exploit}}), \quad (8)$$

$$\text{where } \mathcal{L}(\theta; \mathcal{B}) = \sum_{m=1}^M \sum_{k=1}^K \left(\log \frac{2N P_F(\tau_{\rightarrow x_{m,k}}^{m,k}; \eta(\mathcal{G}_m; \theta), \rho) Z_{\theta}(\mathcal{G}_m)}{R(x_{m,k}; \beta)} \right)^2. \quad (9)$$

The $2N$ comes from the fact that TSP has $2N$ permutations, as discussed in Section 4.2. In addition, our target sampling distribution is proportional to reward $p(x; \mathcal{G}) \propto R(x(\mathcal{G}))$. However, in most

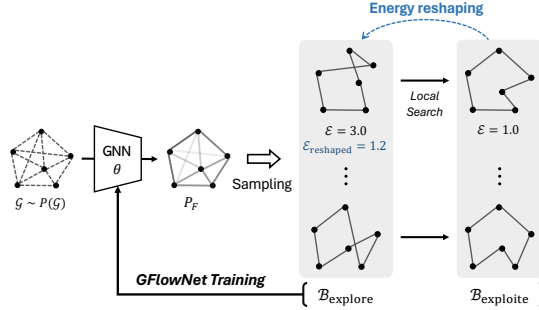


Figure 2: Hindsight observation with local search and energy reshaping to control the trade-off between exploration and exploitation.

COPs, including TSP, the scale of $R(x(\mathcal{G}))$ can vary significantly across instances, possibly leading to unstable training due to the high variance of logarithms of rewards. Similarly to previous works that stabilize REINFORCE training [43, 37], we normalize the energy $\mathcal{E} = -\log R$ using the sample mean over K samples for the same \mathcal{G}_m , i.e.,

$$-\log \tilde{R}(x_{m,k}) = \tilde{\mathcal{E}}(x_{m,k}) = \mathcal{E}(x_{m,k}) - \frac{1}{K} \sum_{k=1}^K \mathcal{E}(x_{m,k}). \quad (10)$$

We call this technique a *shared energy normalization*. Note that the shared energy normalization is applied independently to the two batches, $\mathcal{B}_{\text{explore}}$ and $\mathcal{B}_{\text{exploit}}$, as the energy distribution between the two batches is often significantly different from each other, especially when a heuristic local search is applied. To this end, the gradient loss is computed as follows:

$$\nabla_{\theta} \mathcal{L}(\theta) \approx \nabla_{\theta} \sum_{m=1}^{2M} \sum_{i=1}^I \left(\log \frac{2N P_F(\tau_{\rightarrow x_{i,m}}^{i,m}; \eta(\mathcal{G}_m; \theta), \rho) Z_{\theta}(\mathcal{G}_m; \theta)}{\tilde{R}(x_{i,m})} \right)^2. \quad (11)$$

6 Experiments

This section presents experimental results to validate our algorithm¹. We compare GFACS with other ACO algorithms, and with competitive reinforcement learning algorithms for vehicle routing problems. Moreover, we conduct an ablation study, and perform an empirical comparison with previous GFlowNets training methods, which serve a similar purpose to our method. Below, we provide a brief overview of the experimental setup.

Implementation and hyperparameters. GFACS is built upon the implementation established by DeepACO [79]. As our methodology mainly focuses on improving training algorithms rather than network architecture, we simply adopt the GNN architecture proposed in DeepACO, except the additional parameters for partition function Z_{θ} in Equation (9). For detailed network architecture, hyperparameters and hardware settings, please refer to Appendix A. It is worth noting that one important hyperparameter that GFACS newly introduces is the inverse energy temperature β , which enables us to control the diversity-optimality trade-offs (see Appendix D.2 for detailed analysis). In addition, we employ Ant System [14] for the pheromone updates throughout the experiments, while we also provide experimental results with other ACO variants in Appendix D.3.

Test settings. Each algorithm is tested on the held-out datasets, each with 100 instances generated in advance except TSP, where we obtain the TSP test dataset with 128 instances from Ye et al. [79]. Unless otherwise stated, the results presented throughout this section are the averaged values from three independent models, each trained with a distinct random seed.

6.1 Comparison with ACO algorithms

Here, we compare GFACS against the vanilla ACO with and the DeepACO [79] algorithm across various CO tasks.

Problems. Following the approach of Ye et al. [79], we evaluate our algorithm in a range of COPs. This includes four routing problems – TSP, Capacitated Vehicle Routing Problem (CVRP), CVRP with Time Window (CVRPTW), Prize-Collecting Vehicle Routing Problem (PCTSP), and Orienteering Problem (OP) – along with a scheduling problem – Single Machine Total Weighted Tardiness Problem (SMTWTP) – and a grouping problem, the Bin Packing Problem (BPP). For detailed problem configurations, we direct readers to Appendix B. For TSP, CVRP and CVRPTW, we use local search algorithms with perturbation similar to Ye et al. [79]. For others, we use the destroy-and-repair method (see Appendix C for more details).

Baselines. We use vanilla ACO with a human-designed heuristic matrix, DeepACO as baseline algorithms. We also test GFACS without the proposed off-policy training scheme (called On-policy TB). For inference, we use $K = 100$ ants and $T = 100$ ACO iterations for all the algorithms.

Results. Figure 3 show GFACS consistently outperforms both the classic ACO algorithm and DeepACO across all benchmark problems. Notably, for routing problems, GFACS surpasses DeepACO by a significant margin. This is particularly remarkable given that both algorithms use identical neural networks and local search operators, underscoring the importance of our training strategy.

¹Source code is available: <https://github.com/ai4co/gfacs>.

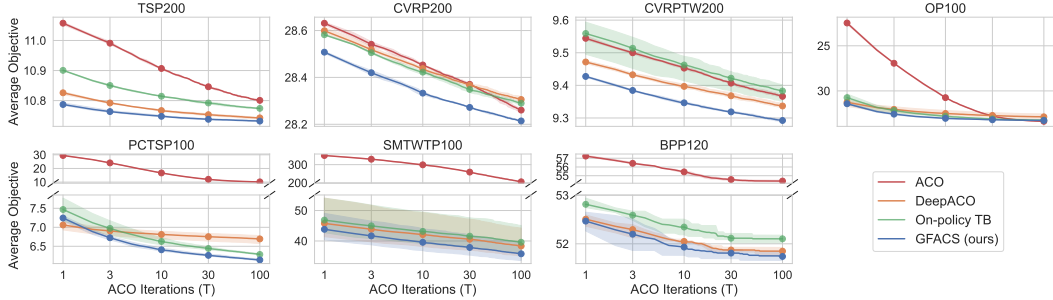


Figure 3: Results of ACO algorithms on various CO tasks. Our GFACS outperforms every ACO baseline. The results are averaged over 3 independent models evaluated on the held-out test sets, and the shade indicates the min-max range of the 3 models.

Table 1: Experimental results on TSP and CVRP. Results for methods with * are drawn from Ye et al. [79], Cheng et al. [8], and Jin et al. [28]. The reported objective value is averaged over 128 instances of TSP and 100 instances of CVRP. We report the average computation time per instance.

Method	TSP500			TSP1000			Method	CVRP500			CVRP1000		
	Obj.	Gap(%)	Time	Obj.	Gap(%)	Time		Obj.	Gap(%)	Time	Obj.	Gap(%)	Time
Concorde	16.55	-	10.7s	23.12	-	108s	PyVRP	62.96	-	21.0m	119.29	-	1.4h
LKH-3	16.55	0.02	31.7s	23.14	0.10	102s	LKH-3	63.07	0.18	18.6m	119.52	0.20	2.1h
AM*	21.46	29.07	0.6s	33.55	45.10	1.5s	POMO	68.69	9.08	2s	145.74	22.14	3s
POMO*	20.57	24.40	0.6s	32.90	42.30	4.1s	+EAS	64.76	2.85	5.0m	126.25	5.83	10.0m
+EAS	18.25	10.29	300s	30.77	33.06	600s	+SGBS	65.44	3.93	5.2m	127.90	7.21	10.1m
+SGBS	18.86	13.98	318s	28.58	23.61	605s	SymNCO	68.81	9.28	2s	141.82	18.86	3s
DIMES*	17.01	2.78	11s	24.45	5.75	32s	+EAS	64.63	2.65	5.0m	125.58	5.27	10.0m
SO*	16.94	2.40	15s	23.77	2.80	26s	+SGBS	65.40	3.87	5.2m	127.53	6.90	10.1m
Pointerformer*	17.14	3.56	14s	24.80	7.90	40s	ACO	64.62	2.63	36s	122.82	2.96	1.3m
ACO	17.38	5.04	14s	24.76	7.09	57s	DeepACO	64.49	2.43	36s	122.15	2.40	1.3m
DeepACO	16.84	1.77	15s	23.78	2.87	66s	GFACS (ours)	64.19	1.95	36s	121.80	2.11	1.3m
GFACS (ours)	16.80	1.56	15s	23.72	2.63	66s							

Additionally, the proposed off-policy training method enhances GFACS performance, demonstrating its effectiveness for GFlowNets.

6.2 Comparison with other reinforcement learning methods for combinatorial optimization

In this section, we present experimental results comparing our method with reinforcement learning (RL)-based approaches, as both aim to develop combinatorial solvers without the need for labeled optimal data points, unlike supervised learning methods (e.g., [16, 70]).

Baselines. For TSP baselines, we select the AM [41], POMO [43], Sym-NCO [37] and Pointerformer [28] as RL-based constructive methods, DIMES [62] as RL-based heatmap-based methods, the Select and Optimize (SO) [9] as RL-based improvement methods. We also applied two search algorithms, the Efficient Active Search (EAS) [23] and Simulation Guided Beam Search (SGBS) [10], to POMO for a more thorough comparison. For CVRP,² we employ POMO and Sym-NCO as baselines with EAS and SGBS. Note that we restrict the duration of these searches to no more than 5 and 10 minutes for problems with 500 and 1000 nodes, respectively. We use Concorde [2] for TSP and PyVRP [77] for CVRP as oracle heuristic solvers to obtain near-optimal solutions that serve as baselines with 0.00% gap. For ACO algorithms, we use 100 ants with $T = 10$ with local search algorithms similar to Ye et al. [79].

Results. Among the baseline methods evaluated, our GFACS algorithm consistently delivers either superior or highly competitive performances. When compared to faster methods like AM or POMO, GFACS demonstrates substantially better results. Even after an additional search with EAS or SGBS, they fail to match GFACS’s performance. Compared to algorithms like DIMES and Pointerformer, which operate at similar speeds, GFACS achieves improved performance. GFACS performs slightly worse than the oracle heuristic solver LKH-3, but offers an advantage of faster inference, especially in CVRP. Therefore, we can conclude that GFACS, as a general-purpose algorithm, holds significant appeal in the highly competitive benchmarks of both TSP and CVRP.

²We also adopt TAM as a CVRP baseline; however, due to the inaccessibility of source code, we compare it using the reported result in the paper [24]. See Appendix D.5.

Table 2: Experimental results on real-world datasets, TSPLib and CVRPLib-X. ‘#’ denotes the number of instances in each set. We report the average optimality gap using the best-known costs.

TSPLib	#	ACO	DeepACO	Ours	CVRPLib-X	#	ACO	DeepACO	Ours
100-299	30	1.71%	1.25%	1.21%	100-299	43	2.50%	3.27%	2.69%
300-699	10	4.26%	2.70%	2.60%	300-699	40	3.75%	4.22%	3.71%
700-1499	12	7.01%	4.08%	3.88%	700-1001	17	4.64%	5.07%	4.32%

Evaluation on real-world datasets. We compare the performance of our model against baseline models on real-world TSP and CVRP instances from the TSPLib [64] and CVRPLib [72] X datasets. The models were trained on random uniform instances of TSP/CVRP with sizes 200 for dataset sizes 100-299, 500 for sizes 300-699, and 1000 for sizes 700-1499, with all other settings remaining the same. Table 2 presents the results. GFACS outperforms the baselines in TSPLib and large CVRPLib instances but slightly underperforms compared to vanilla ACO on small CVRPLib instances, where ACO with Swap* local search suffices for small-scale CVRP. As the problem scale increases, ACO’s performance declines, underscoring the importance of effective priors using GFlowNets for efficient pheromone posterior updates in large combinatorial spaces.

6.3 Ablation study

This section reports the ablation study results, validating our proposed training techniques for stabilizing and enhancing GFlowNets in large-scale combinatorial optimization tasks. As detailed in Table 3, our off-policy training method, incorporating local search, energy reshaping to value potential solutions, and shared ϵ -norm to stabilize conditional GFlowNets training, significantly improves performance across three tasks: TSP, CVRP, and BPP. For comprehensive results, please refer to Table 10.

Table 3: Results of the ablation study for the proposed training techniques.

Method	TSP500	CVRP500	BPP120
GFACS	16.80	64.19	51.84
– Off-policy Training	17.09	64.42	52.32
– Energy Reshaping	16.87	64.41	52.07
– Shared ϵ -norm	17.52	65.51	90.73
+ VarGrad [82]	16.86	64.28	51.95

6.4 Comparative analysis with previous GFlowNets training methods

While this paper proposes a novel training method for GFlowNets designed for large-scale combinatorial optimization problems that are not locally decomposable due to their cyclic nature (e.g., TSP, CVRP) [1], we also compare existing GFlowNets training methods within this domain.

Forward-looking detailed balance (FL-DB) [59, 84]. FL-DB leverages local credits when the application benefits from useful local rewards for partial solutions. While graph combinatorial optimization tasks are generally locally decomposable [1], yielding useful local rewards, tasks like TSP do not offer substantial local rewards due to their cyclic nature, which imposes a global constraint, thus complicating local credit assignment. As shown in Figure 4, various GFlowNet methods were used to train the ACO’s heuristic matrix $\eta(\mathcal{G}; \theta)$. While FL-DB did not surpass on-policy TB for TSP, our off-policy method demonstrated significant improvement. This trend holds across different deep learning models and inference tasks beyond ACO (see Appendix D.1).

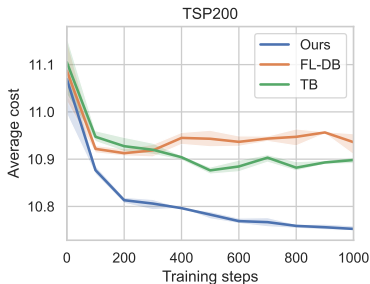


Figure 4: Validation costs during training with different GFlowNet losses.

Gradient of log-partition variance (VarGrad) [65, 82]. The VarGrad loss, initially proposed by Richter et al. [65] for variational inference, was applied to conditional GFlowNets for solving scheduling problems by Zhang et al. [82]. This approach is crucial for combinatorial optimization tasks that require conditional inference on problem instances (\mathcal{G}). The key idea involves using a generative distribution and energy to compute the log-partition function through the consistency property of log-partitions over trajectories conditioned on identical instances (\mathcal{G}), thereby bypassing the explicit training of the (conditional) log-partition ($\log Z(\mathcal{G})$). Explicit training of the log-partition is challenging in conditional GFlowNets due to the varying energy landscapes across different instance conditions (\mathcal{G}). On the other hand, our method, which utilizes explicit training of the log-partition (see Equation (9)), outperforms VarGrad in training conditional GFlowNets (see Table 3).

This improvement is achieved because our *Share ϵ -norms* enable stable and explicit training of the log-partition by normalizing energy values into sample means, resulting in an energy distribution across different instances that maintains a mean of zero. Note that accurately estimated the explicit log-partition value is known to stabilize the amortized inference process in GFlowNets [53].

7 Discussion

This paper proposes a novel probabilistic search method leveraging the off-policy training capabilities of GFlowNets. This strategy can be applied not only to ant-colony optimization (ACO) but also to other probabilistic methods requiring an effective learned prior (see Appendix D.4). Our off-policy framework enables the integration of learning algorithms with offline datasets containing optimal combinatorial solutions for specific problem instances, combined with online exploration to fine-tune the policy through off-to-on training. This approach holds promise for future work.

Limitation. A limitation of our method is that its performance depends on the effectiveness of the local search. A promising future direction could involve leveraging advanced neural-guided improvement heuristics, including neural local search approaches [48, 50], to create a hybrid algorithm that combines GFlowNets with neural improvement-based local search.

References

- [1] Sungsoo Ahn, Younggyo Seo, and Jinwoo Shin. Learning what to defer for maximum independent sets. In *International Conference on Machine Learning*, pages 134–144. PMLR, 2020.
- [2] David Applegate, Robert Bixby, Vasek Chvatal, and William Cook. Concorde TSP solver, 2006. URL <https://www.math.uwaterloo.ca/tsp/concorde/>.
- [3] Irwan Bello, Hieu Pham, Quoc V Le, Mohammad Norouzi, and Samy Bengio. Neural combinatorial optimization with reinforcement learning. *arXiv preprint arXiv:1611.09940*, 2016.
- [4] Emmanuel Bengio, Moksh Jain, Maksym Korablyov, Doina Precup, and Yoshua Bengio. Flow network based generative models for non-iterative diverse candidate generation. In *Advances in Neural Information Processing Systems*, volume 34, pages 27381–27394, 2021.
- [5] Yoshua Bengio, Salem Lahlou, Tristan Deleu, Edward J Hu, Mo Tiwari, and Emmanuel Bengio. Gflownet foundations. *Journal of Machine Learning Research*, 24(210):1–55, 2023.
- [6] Federico Berto, Chuanbo Hua, Junyoung Park, Minsu Kim, Hyeonah Kim, Jiwoo Son, Haeyeon Kim, Joungho Kim, and Jinkyoo Park. RL4CO: a unified reinforcement learning for combinatorial optimization library. In *NeurIPS 2023 Workshop: New Frontiers in Graph Learning*, 2023.
- [7] Felix Chalumeau, Shikha Surana, Clément Bonnet, Nathan Grinsztajn, Arnu Pretorius, Alexandre Larterre, and Tom Barrett. Combinatorial optimization with policy adaptation using latent space search. In *Advances in Neural Information Processing Systems*, volume 36, pages 7947–7959, 2023.
- [8] Hanni Cheng, Haosi Zheng, Ya Cong, Weihao Jiang, and Shiliang Pu. Select and optimize: Learning to solve large-scale tsp instances. In *International Conference on Artificial Intelligence and Statistics*, pages 1219–1231. PMLR, 2023.
- [9] Hanni Cheng, Haosi Zheng, Ya Cong, Weihao Jiang, and Shiliang Pu. Select and optimize: Learning to solve large-scale tsp instances. In *International Conference on Artificial Intelligence and Statistics*, volume 206, pages 1219–1231. PMLR, 25–27 Apr 2023.
- [10] Jinho Choo, Yeong-Dae Kwon, Jihoon Kim, Jeongwoo Jae, André Hottung, Kevin Tierney, and Youngjune Gwon. Simulation-guided beam search for neural combinatorial optimization. In *Advances in Neural Information Processing Systems*, volume 35, pages 8760–8772, 2022.
- [11] A. Croes. A method for solving traveling salesman problems. *Operations Research*, 5:791–812, 1958.

- [12] Paulo R d O Costa, Jason Rhuggenaath, Yingqian Zhang, and Alp Akcay. Learning 2-opt heuristics for the traveling salesman problem via deep reinforcement learning. In *Asian Conference on Machine Learning*, pages 465–480. PMLR, 2020.
- [13] Tristan Deleu, Padideh Nouri, Nikolay Malkin, Doina Precup, and Yoshua Bengio. Discrete probabilistic inference as control in multi-path environments. *arXiv preprint arXiv:2402.10309*, 2024.
- [14] M. Dorigo, V. Maniezzo, and A. Coloni. Ant system: optimization by a colony of cooperating agents. *IEEE Transactions on Systems, Man, and Cybernetics, Part B (Cybernetics)*, 26(1): 29–41, 1996. doi: 10.1109/3477.484436.
- [15] Marco Dorigo, Mauro Birattari, and Thomas Stutzle. Ant colony optimization. *IEEE Computational Intelligence Magazine*, 1(4):28–39, 2006. doi: 10.1109/MCI.2006.329691.
- [16] Darko Drakulic, Sofia Michel, Florian Mai, Arnaud Sors, and Jean-Marc Andreoli. BQ-NCO: Bisimulation quotienting for efficient neural combinatorial optimization. In *Advances in Neural Information Processing Systems*, volume 36, pages 77416–77429, 2023.
- [17] Stefan Elfwing, Eiji Uchibe, and Kenji Doya. Sigmoid-weighted linear units for neural network function approximation in reinforcement learning. *Neural Networks*, 107:3–11, 2018.
- [18] E. Falkenauer and A. Delchambre. A genetic algorithm for bin packing and line balancing. In *IEEE International Conference on Robotics and Automation*, volume 2, pages 1186–1192, 1992. doi: 10.1109/ROBOT.1992.220088.
- [19] Matteo Fischetti, Juan Jose Salazar Gonzalez, and Paolo Toth. Solving the orienteering problem through branch-and-cut. *INFORMS Journal on Computing*, 10(2):133–148, 1998.
- [20] Zhang-Hua Fu, Kai-Bin Qiu, and Hongyuan Zha. Generalize a small pre-trained model to arbitrarily large tsp instances. In *Proceedings of the AAAI Conference on Artificial Intelligence*, volume 35, pages 7474–7482, 2021.
- [21] Nathan Grinsztajn, Daniel Furelos-Blanco, and Thomas D Barrett. Population-based reinforcement learning for combinatorial optimization. *arXiv preprint arXiv:2210.03475*, 2022.
- [22] André Hottung and Kevin Tierney. Neural large neighborhood search for the capacitated vehicle routing problem. In *ECAI 2020*, pages 443–450. IOS Press, 2020.
- [23] André Hottung, Yeong-Dae Kwon, and Kevin Tierney. Efficient active search for combinatorial optimization problems. In *International Conference on Learning Representations*, 2022.
- [24] Qingchun Hou, Jingwei Yang, Yiqiang Su, Xiaoqing Wang, and Yuming Deng. Generalize learned heuristics to solve large-scale vehicle routing problems in real-time. In *International Conference on Learning Representations*, 2023.
- [25] Sergey Ioffe and Christian Szegedy. Batch normalization: Accelerating deep network training by reducing internal covariate shift. In *International Conference on Machine Learning*, pages 448–456. PMLR, 2015.
- [26] Hyosoon Jang, Minsu Kim, and Sungsoo Ahn. Learning energy decompositions for partial inference of GFlowNets. *International Conference on Learning Representations*, 2024.
- [27] YUAN JIANG, Zhiguang Cao, Yaoxin Wu, Wen Song, and Jie Zhang. Ensemble-based deep reinforcement learning for vehicle routing problems under distribution shift. In *Advances in Neural Information Processing Systems*, volume 36, pages 53112–53125, 2023.
- [28] Yan Jin, Yuandong Ding, Xuanhao Pan, Kun He, Li Zhao, Tao Qin, Lei Song, and Jiang Bian. Pointerformer: Deep reinforced multi-pointer transformer for the traveling salesman problem. In *Proceedings of the AAAI Conference on Artificial Intelligence*, volume 37, pages 8132–8140, 2023.
- [29] Chaitanya K Joshi, Quentin Cappart, Louis-Martin Rousseau, and Thomas Laurent. Learning TSP requires rethinking generalization. In *International Conference on Principles and Practice of Constraint Programming*, 2021.

- [30] Elias Khalil, Hanjun Dai, Yuyu Zhang, Bistra Dilkina, and Le Song. Learning combinatorial optimization algorithms over graphs. In *Advances in Neural Information Processing Systems*, volume 30, 2017.
- [31] Haeyeon Kim, Minsu Kim, Federico Berto, Joungho Kim, and Jinkyoo Park. Devformer: A symmetric transformer for context-aware device placement. In *International Conference on Machine Learning*, pages 16541–16566. PMLR, 2023.
- [32] Hyeonah Kim, Minsu Kim, Sungsoo Ahn, and Jinkyoo Park. Symmetric Replay Training: Enhancing sample efficiency in deep reinforcement learning for combinatorial optimization. In *International Conference on Machine Learning*, 2024.
- [33] Minjun Kim, Junyoung Park, and Jinkyoo Park. Learning to CROSS exchange to solve min-max vehicle routing problems. In *International Conference on Learning Representations*, 2023.
- [34] Minsu Kim, Hyunwook Park, Seongguk Kim, Keeyoung Son, Subin Kim, Kyunjune Son, Seonguk Choi, Gapyeol Park, and Joungho Kim. Reinforcement learning-based auto-router considering signal integrity. In *2020 IEEE 29th Conference on Electrical Performance of Electronic Packaging and Systems (EPEPS)*, pages 1–3, 2020. doi: 10.1109/EPEPS48591.2020.9231473.
- [35] Minsu Kim, Hyunwook Park, Keeyoung Son, Seongguk Kim, Haeyeon Kim, Jihun Kim, Jinwook Song, Youngmin Ku, Joungho Kim, and Joungho Kim. Imitation learning for simultaneous escape routing. In *2021 IEEE 30th Conference on Electrical Performance of Electronic Packaging and Systems (EPEPS)*, pages 1–3, 2021. doi: 10.1109/EPEPS51341.2021.9609145.
- [36] Minsu Kim, Jinkyoo Park, and Joungho Kim. Learning collaborative policies to solve np-hard routing problems. In *Advances in Neural Information Processing Systems*, volume 34, pages 10418–10430, 2021.
- [37] Minsu Kim, Junyoung Park, and Jinkyoo Park. Sym-NCO: Leveraging symmetry for neural combinatorial optimization. In *Advances in Neural Information Processing Systems*, volume 35, pages 1936–1949, 2022.
- [38] Minsu Kim, Joohwan Ko, Taeyoung Yun, Dinghuai Zhang, Ling Pan, Woochang Kim, Jinkyoo Park, Emmanuel Bengio, and Yoshua Bengio. Learning to scale logits for temperature-conditional GFlowNets. In *International Conference on Machine Learning*, 2024.
- [39] Minsu Kim, Taeyoung Yun, Emmanuel Bengio, Dinghuai Zhang, Yoshua Bengio, Sungsoo Ahn, and Jinkyoo Park. Local search GFlowNets. In *International Conference on Learning Representations*, 2024.
- [40] Thomas N Kipf and Max Welling. Semi-supervised classification with graph convolutional networks. *arXiv preprint arXiv:1609.02907*, 2016.
- [41] Wouter Kool, Herke van Hoof, and Max Welling. Attention, learn to solve routing problems! In *International Conference on Learning Representations*, 2019.
- [42] Wouter Kool, Herke van Hoof, Joaquim Gromicho, and Max Welling. Deep policy dynamic programming for vehicle routing problems. In *International Conference on Integration of Constraint Programming, Artificial Intelligence, and Operations Research*, pages 190–213. Springer, 2022.
- [43] Yeong-Dae Kwon, Jinho Choo, Byoungjip Kim, Iljoo Yoon, Youngjune Gwon, and Seungjai Min. POMO: Policy optimization with multiple optima for reinforcement learning. In *Advances in Neural Information Processing Systems*, volume 33, pages 21188–21198, 2020.
- [44] Yang Li, Jinpei Guo, Runzhong Wang, and Junchi Yan. From distribution learning in training to gradient search in testing for combinatorial optimization. In *Thirty-seventh Conference on Neural Information Processing Systems*, 2023. URL <https://openreview.net/forum?id=JtF0ugNMv2>.

- [45] Ilya Loshchilov and Frank Hutter. SGDR: Stochastic gradient descent with warm restarts. In *International Conference on Learning Representations*, 2017.
- [46] Ilya Loshchilov and Frank Hutter. Decoupled weight decay regularization. *arXiv preprint arXiv:1711.05101*, 2017.
- [47] Fu Luo, Xi Lin, Fei Liu, Qingfu Zhang, and Zhenkun Wang. Neural combinatorial optimization with heavy decoder: Toward large scale generalization. In *Advances in Neural Information Processing Systems*, volume 36, pages 8845–8864, 2023.
- [48] Yining Ma, Jingwen Li, Zhiguang Cao, Wen Song, Le Zhang, Zhenghua Chen, and Jing Tang. Learning to iteratively solve routing problems with dual-aspect collaborative Transformer. In *Advances in Neural Information Processing Systems*, volume 34, pages 11096–11107, 2021.
- [49] Yining Ma, Jingwen Li, Zhiguang Cao, Wen Song, Hongliang Guo, Yuejiao Gong, and Meng Chee Chee. Efficient neural neighborhood search for pickup and delivery problems. In *International Joint Conference on Artificial Intelligence*, pages 23–29, 2022.
- [50] Yining Ma, Zhiguang Cao, and Yeow Meng Chee. Learning to search feasible and infeasible regions of routing problems with flexible neural k-opt. In *Advances in Neural Information Processing Systems*, volume 36, pages 49555–49578, 2023.
- [51] Kanika Madan, Jarrid Rector-Brooks, Maksym Korablyov, Emmanuel Bengio, Moksh Jain, Andrei Nica, Tom Bosc, Yoshua Bengio, and Nikolay Malkin. Learning GFlowNets from partial episodes for improved convergence and stability. In *International Conference on Machine Learning*, pages 23467–23483. PMLR, 2023.
- [52] Nikolay Malkin, Moksh Jain, Emmanuel Bengio, Chen Sun, and Yoshua Bengio. Trajectory balance: Improved credit assignment in GFlowNets. In *Advances in Neural Information Processing Systems*, volume 35, pages 5955–5967, 2022.
- [53] Nikolay Malkin, Salem Lahlou, Tristan Deleu, Xu Ji, Edward Hu, Katie Everett, Dinghuai Zhang, and Yoshua Bengio. GFlowNets and variational inference. In *International Conference on Learning Representations*, 2023.
- [54] Yimeng Min, Yiwei Bai, and Carla P Gomes. Unsupervised learning for solving the travelling salesman problem. In *Advances in Neural Information Processing Systems*, volume 36, pages 47264–47278, 2023.
- [55] Volodymyr Mnih, Koray Kavukcuoglu, David Silver, Alex Graves, Ioannis Antonoglou, Daan Wierstra, and Martin Riedmiller. Playing atari with deep reinforcement learning. *arXiv preprint arXiv:1312.5602*, 2013.
- [56] Sobhan Mohammadpour, Emmanuel Bengio, Emma Frejinger, and Pierre-Luc Bacon. Maximum entropy GFlowNets with soft Q-learning. In *International Conference on Artificial Intelligence and Statistics*, pages 2593–2601. PMLR, 2024.
- [57] MohammadReza Nazari, Afshin Oroojlooy, Lawrence Snyder, and Martin Takac. Reinforcement learning for solving the vehicle routing problem. In *Advances in Neural Information Processing Systems*, volume 31, 2018.
- [58] Ling Pan, Dinghuai Zhang, Aaron Courville, Longbo Huang, and Yoshua Bengio. Generative augmented flow networks. In *International Conference on Learning Representations*, 2022.
- [59] Ling Pan, Nikolay Malkin, Dinghuai Zhang, and Yoshua Bengio. Better training of GFlowNets with local credit and incomplete trajectories. In *International Conference on Machine Learning*, pages 26878–26890. PMLR, 23–29 Jul 2023.
- [60] Hyunwook Park, Minsu Kim, Seongguk Kim, Keunwoo Kim, Haeyeon Kim, Taein Shin, Keeyoung Son, Boogyo Sim, Subin Kim, Seungtaek Jeong, Chulsoon Hwang, and Joungho Kim. Transformer network-based reinforcement learning method for power distribution network (PDN) optimization of high bandwidth memory (HBM). *IEEE Transactions on Microwave Theory and Techniques*, 70(11):4772–4786, 2022. doi: 10.1109/TMTT.2022.3202221.

- [61] David Pisinger and Stefan Ropke. Large neighborhood search. *Handbook of metaheuristics*, pages 99–127, 2019.
- [62] Ruizhong Qiu, Zhiqing Sun, and Yiming Yang. DIMES: A differentiable meta solver for combinatorial optimization problems. In *Advances in Neural Information Processing Systems*, volume 35, pages 25531–25546, 2022.
- [63] Jarrid Rector-Brooks, Kanika Madan, Moksh Jain, Maksym Korablyov, Cheng-Hao Liu, Sarath Chandar, Nikolay Malkin, and Yoshua Bengio. Thompson sampling for improved exploration in GFlowNets. *arXiv preprint arXiv:2306.17693*, 2023.
- [64] Gerhard Reinelt. TSPLIB—A traveling salesman problem library. *ORSA journal on computing*, 3(4):376–384, 1991.
- [65] Lorenz Richter, Ayman Boustati, Nikolas Nüsken, Francisco Ruiz, and Omer Deniz Akyildiz. Vargrad: A low-variance gradient estimator for variational inference. In *Advances in Neural Information Processing Systems*, volume 33, pages 13481–13492, 2020.
- [66] Jiwoo Son, Minsu Kim, Hyeonah Kim, and Jinkyoo Park. Meta-SAGE: scale meta-learning scheduled adaptation with guided exploration for mitigating scale shift on combinatorial optimization. In *International Conference on Machine Learning*, pages 32194–32210. PMLR, 2023.
- [67] Jiwoo Son, Minsu Kim, Sanghyeok Choi, Hyeonah Kim, and Jinkyoo Park. Equity-Transformer: Solving np-hard min-max routing problems as sequential generation with equity context. In *Proceedings of the AAAI Conference on Artificial Intelligence*, volume 38, pages 20265–20273, 2024.
- [68] Thomas Stützle and Holger H. Hoos. MAX–MIN ant system. *Future Generation Computer Systems*, 16(8):889–914, 2000. ISSN 0167-739X. doi: [https://doi.org/10.1016/S0167-739X\(00\)00043-1](https://doi.org/10.1016/S0167-739X(00)00043-1). URL <https://www.sciencedirect.com/science/article/pii/S0167739X00000431>.
- [69] Haoran Sun, Katayoon Goshvadi, Azade Nova, Dale Schuurmans, and Hanjun Dai. Revisiting sampling for combinatorial optimization. In *International Conference on Machine Learning*, volume 202, pages 32859–32874. PMLR, 23–29 Jul 2023.
- [70] Zhiqing Sun and Yiming Yang. DIFUSCO: Graph-based diffusion solvers for combinatorial optimization. In *Advances in Neural Information Processing Systems*, volume 36, pages 3706–3731, 2023.
- [71] Richard S Sutton, David McAllester, Satinder Singh, and Yishay Mansour. Policy gradient methods for reinforcement learning with function approximation. *Advances in neural information processing systems*, 12, 1999.
- [72] Eduardo Uchoa, Diego Pecin, Artur Pessoa, Marcus Poggi, Thibaut Vidal, and Anand Subramanian. New benchmark instances for the capacitated vehicle routing problem. *European Journal of Operational Research*, 257(3):845–858, 2017.
- [73] Petar Veličković, Guillem Cucurull, Arantxa Casanova, Adriana Romero, Pietro Liò, and Yoshua Bengio. Graph attention networks. In *International Conference on Learning Representations*, 2018.
- [74] Thibaut Vidal. Hybrid genetic search for the cvrp: Open-source implementation and swap* neighborhood. *Computers & Operations Research*, 140:105643, 2022.
- [75] Oriol Vinyals, Meire Fortunato, and Navdeep Jaitly. Pointer networks. In *Advances in Neural Information Processing Systems*, volume 28, 2015.
- [76] Ronald J Williams. Simple statistical gradient-following algorithms for connectionist reinforcement learning. *Machine learning*, 8:229–256, 1992.
- [77] Niels A. Wouda, Leon Lan, and Wouter Kool. PyVRP: a high-performance VRP solver package. *INFORMS Journal on Computing*, 2024. doi: 10.1287/ijoc.2023.0055. URL <https://doi.org/10.1287/ijoc.2023.0055>.

- [78] Liang Xin, Wen Song, Zhiguang Cao, and Jie Zhang. Multi-decoder attention model with embedding glimpse for solving vehicle routing problems. In *Proceedings of the AAAI Conference on Artificial Intelligence*, volume 35, pages 12042–12049, 2021.
- [79] Haoran Ye, Jiarui Wang, Zhiguang Cao, Helan Liang, and Yong Li. DeepACO: Neural-enhanced ant systems for combinatorial optimization. In *Advances in Neural Information Processing Systems*, volume 36, pages 43706–43728, 2023.
- [80] Haoran Ye, Jiarui Wang, Helan Liang, Zhiguang Cao, Yong Li, and Fanzhang Li. GLOP: Learning global partition and local construction for solving large-scale routing problems in real-time. In *Proceedings of the AAAI Conference on Artificial Intelligence*, volume 38, pages 20284–20292, 2024.
- [81] Cong Zhang, Wen Song, Zhiguang Cao, Jie Zhang, Puay Siew Tan, and Xu Chi. Learning to dispatch for job shop scheduling via deep reinforcement learning. In *Advances in Neural Information Processing Systems*, volume 33, pages 1621–1632, 2020.
- [82] David W Zhang, Corrado Rainone, Markus Peschl, and Roberto Bondesan. Robust scheduling with GFlowNets. In *International Conference on Learning Representations*, 2022.
- [83] Dinghuai Zhang, Nikolay Malkin, Zhen Liu, Alexandra Volokhova, Aaron Courville, and Yoshua Bengio. Generative flow networks for discrete probabilistic modeling. In *International Conference on Machine Learning*, pages 26412–26428. PMLR, 2022.
- [84] Dinghuai Zhang, Hanjun Dai, Nikolay Malkin, Aaron C Courville, Yoshua Bengio, and Ling Pan. Let the flows tell: Solving graph combinatorial problems with gflownets. In *Advances in Neural Information Processing Systems*, volume 36, 2023.
- [85] Dinghuai Zhang, L. Pan, Ricky T. Q. Chen, Aaron C. Courville, and Yoshua Bengio. Distributional GFlowNets with quantile flows. *Transactions on Machine Learning Research*, 2024.
- [86] Jianan Zhou, Zhiguang Cao, Yaoxin Wu, Wen Song, Yining Ma, Jie Zhang, and Chi Xu. MV-MoE: Multi-task vehicle routing solver with mixture-of-experts. In *International Conference on Machine Learning*, 2024.

A Implementation

A.1 Learning architecture and optimizer

We utilize the anisotropic graph neural network with edge gating mechanisms, which is proposed by [29] and adopted by [79], as the foundational GNN architecture for the construction of a heuristic matrix. This network offers node and edge embeddings that are more beneficial for edge prediction than other popular GNN variants, such as Graph Attention Networks [73] or Graph Convolutional Networks [40].

We represent the node feature of node v_i at the ℓ -th layer as h_i^ℓ , and the feature of the edge between nodes i and j at the same layer as e_{ij}^ℓ . These features undergo propagation to the next layer $\ell + 1$ through an anisotropic message passing scheme, detailed as follows:

$$h_i^{\ell+1} = h_i^\ell + \text{ACT}(\text{BN}(U^\ell h_i^\ell + \mathcal{A}_{j \in \mathcal{N}_i}(\sigma(e_{ij}^\ell) \odot V^\ell h_j^\ell))) \quad (12)$$

$$m^\ell = P^\ell e_{ij}^\ell + Q^\ell h_i^\ell + R^\ell h_j^\ell \quad (13)$$

$$e_{ij}^{\ell+1} = e_{ij}^\ell + \text{ACT}(\text{BN}(m^\ell)) \quad (14)$$

where $U^\ell, V^\ell, P^\ell, Q^\ell, R^\ell \in R^{d \times d}$ are the learnable parameters of layer ℓ , ACT denotes the activation function, BN[25] denotes batch normalization, \mathcal{A} denote the aggregation function, σ is the sigmoid function, \odot is Hadamard product, \mathcal{N}_i denotes the neighborhoods of node v_i . In this paper we use α is SiLU[17] and \mathcal{A} is mean pooling. We transform the extracted edge features into real-valued heuristic metrics by employing a 3-layer Multilayer Perceptron (MLP) that includes skipping connections to the embedded node feature h . The SiLU is the activation function for all layers except the output layer, in which the sigmoid function is applied to generate normalized outputs. The training process is optimized using the AdamW optimizer[46] in conjunction with a Cosine Annealing Scheduler[45]

A.2 Hyperparameters

Table 4: Training hyperparameter settings for each task. These hyperparameter settings are used both for GFACS and DeepACO training. The values with * indicate that the values are used for fine-tuning a pre-trained model.

	TSP200	TSP500	TSP1000	CVRP200	CVRP500	CVRP1000	OP100	PCTSP100	SMTWTP100	BPP120
N_{epoch}	50	50	20*	50	50	20*	20	20	20	20
N_{inst}	400	400	200*	200	200	100*	100	100	100	100
M	20	20	10	10	10	5	5	5	5	5
K	30	30	20	20	20	15	30	30	30	30

For a task of COP (e.g., TSP200), we train GFACS for N_{epoch} epochs. In each epoch, we use N_{inst} number of instances using mini-batch with size M ; thus N_{inst}/M gradient steps are taken per epoch. For each problem instance, we sample K solutions to train with, as discussed in Section 5.1. Our main baseline algorithm, DeepACO, is also trained using the same hyperparameters to ensure a fair comparison. We summarize used value for N_{epoch} , N_{inst} , M and K in Table 4. Note that for TSP1000 and CVRP1000, we use model checkpoints pre-trained in TSP500 and CVRP500, respectively, to reduce the processing time for training.

There are other hyperparameters to be considered specifically for GFACS. β is one of the most important hyperparameters for training GFACS, which is analyzed in Appendix D.2. We use annealing for β using the following log-shaped scheduling:

$$\beta = \beta_{\min} + (\beta_{\max} - \beta_{\min}) \min \left(\frac{\log(i_{\text{epoch}})}{\log(N_{\text{epoch}} - N_{\text{flat}})}, 1 \right)$$

where i_{epoch} is the index of epoch and N_{flat} is the number of last epochs to have $\beta = \beta_{\max}$.

We report the β value used for each task in Table 5. Note that β remains consistent across different scales of the same problem class.

Table 5: Settings of β for each task.

	TSP	CVRP	CVRPTW	OP	PCTSP	SMTWTP	BPP
β_{\min}	200	500	500	5	20	10	1000
β_{\max}	1000	2000	2000	10	50	20	2000

For TSP and CVRP, where we have local search operators, we also need α for energy reshaping (Eq. 7). We empirically found that linearly increasing α from 0.5 to 1.0 along the epochs works well, and we use that setting for all TSP and CVRP experiments.

A.3 Computing resource

Throughout the experiments, we utilize a single CPU, specifically an AMD EPYC 7542 32-Core Processor, and a single GPU, the NVIDIA RTX A6000, for training neural networks. After that, the inference was conducted on a separate, standalone PC with a single AMD Ryzen 9 5900X 12-Core Processor and NVIDIA RTX 4070 Ti to assess the wall time of each algorithm fairly.

B Problem settings

In this section, we provide an overview of the combinatorial optimization problems we address. These encompass vehicle routing problems, bin packing problems, and scheduling problems. For a comprehensive understanding of each problem’s specific settings, we direct readers to the work by Ye et al. [79]. Furthermore, for access to the exact source code pertaining to each problem, please refer to the repository available at ³ from Ye et al. [79].

Traveling salesman problem In the traveling salesman problem (TSP), we aim to find the shortest route that visits a set of nodes once and returns to the origin. We consider Euclidean TSP, where the distance between two nodes is determined by Euclidean distance. A TSP instance can be determined as a set of nodes with 2D coordinates. We generate a random TSP instance by sampling the coordinate from a unit square, $[0, 1]^2$.

Capacitated vehicle routing problem Similar to TSP, capacitated vehicle routing problem (CVRP) also seeks the shortest path that visits all the nodes once. In CVRP, however, a vehicle has a limited capacity, and each node has a demand to be satisfied. The sum of the demand of each subroute should not exceed the capacity, which limits the number of nodes that can be visited by one vehicle. In our setting, CVRP is also defined in Euclidean space.

A CVRP instance can be represented by a set of customer nodes, a single depot node, and a capacity C . Each customer node has a position (2D coordinates) and a demand, while the depot only has a position. A random CVRP instance is generated by sampling the coordinates of both customer and depot from a unit square $[0, 1]^2$ and sampling demands for each customer from a predefined uniform distribution, $U[a, b]$. We use $a = 1$ and $b = 9$, and a fixed $C = 50$ for all problem scales, 200, 500 and 1000.

Capacitated vehicle routing problem with time window A uniform-capacity fleet of delivery vehicles is tasked with servicing customers who have specific demand and operating hours (earliest-latest arrival) for a single commodity. The vehicles should deliver to customer only the time available for service. The goals are to minimize the total travel distance.

A CVRPTW instance consists of a set of customer nodes, a single depot node, the demands of each customer node, the vehicle capacity (as in CVRP), and additionally, the earliest and latest arrival times for each node, as well as the service time at each node. We generate the CVRPTW instance following the method provided by Berto et al. [6], which can be accessed here⁴.

³<https://github.com/henry-yeh/DeepACO>

⁴<https://github.com/ai4co/rl4co/blob/main/rl4co/envs/routing/cvrptw/generator.py>

Orienteering problem In the orienteering problem (OP), the objective is to maximize the total prize of visited nodes within a given tour length limitation. This problem is similar to CVRP but focuses on maximizing gains rather than minimizing costs.

An OP instance comprises a set of nodes to visit, each with its position and prize, a depot, and a maximum length constraint. We sample a random OP instance by first sampling the position of nodes, including the starting node, from a unit square $[0, 1]^2$. And we set the prize for each node, following [19, 79], to be $p_i = (1 + \lfloor 99 \cdot \frac{d_{0,i}}{\max_{j=1}^n d_{0,j}} \rfloor) / 100$, where $d_{0,i}$ is the Euclidean distance from the depot to node i . We set the maximum length to 4 in the OP100 task, following Kool et al. [41].

Prize-collecting traveling salesman problem The prize-collecting traveling salesman problem (PCTSP) extends the TSP by associating a prize for visiting a node and a penalty for not visiting it. The goal is to find a tour that minimizes the total travel cost plus penalties for the unvisited nodes and also satisfies a predefined prize threshold. In PCTSP, balancing the need to collect prizes against the cost of visiting more nodes matters.

A PCTSP instance comprises a set of nodes to visit, a depot, and a minimum total prize threshold. The coordinates of nodes and depot are sampled in the unit square. The prize for each node is sampled from $U[0, 1]$, while the penalty for each node is sampled from $U[0, C_N]$, where C_N is set to 0.12 for $N = 100$. Lastly, the minimum total prize threshold is $N/4$ for problems with N nodes, i.e., 25 for PCTSP100.

Single machine total weighted tardiness problem This problem involves scheduling jobs on a single machine where each job has a due date, processing time, and weight. The objective is to minimize the total weighted tardiness, which is the sum of the weights of the jobs multiplied by their tardiness (the amount of time a job is completed after its due date).

To generate an SMTWTP instance, we sample a due date from $U[0, N]$, the weight from $U[0, 1]$, and the processing time from $U[0, 2]$, where N is the number of jobs to process.

Bin packing problem The bin packing problem (BPP) aims to minimize the number of bins when objects with different volumes need to be packed into a finite number of bins. The cost functions are often modified to maximize the utility of used bins [18, 79]. However, the direct use of the objective function employed in DeepACO can lead to an excessively large β since the objective values tend to be saturated near 1.0; note that the objective values can not exceed 1.0 in that setting. Therefore, we slightly modify them to minimize a weighted sum of the inverse of the utilization of the used bins throughout all our BPP experiments.

To generate a BPP instance, we sample the N items with a random size from $U[20, 100]$. And we use 150 for the bin capacity.

C Implementation of destroy-and-repair local search

As demonstrated in Section 5, our algorithm utilizes the local search for off-policy training. The refined solutions from local search serve as exploitation batches, and they are also used for energy-reshaping (Eq. 7). For some problems like traveling salesman problem (TSP), capacitated vehicle routing problem (CVRP), and CVRP with time window (CVRPTW), we used the well-established local search operators such as 2-opt, Swap* [74] and granular neighborhood search from PyVRP [77].

While domain-specific local search techniques are well developed for many combinatorial optimization problems, there are still tasks that lack effective local search solvers like Swap*. A potential candidate for a general-purpose local search solver in combinatorial optimization is the destroy-and-reconstruct local search operator. This method is inspired by the large neighborhood search approach described by Pisinger and Ropke [61]. Our implementation utilizes an evolutionary-style algorithm that repeatedly performs destruction, reconstruction, and top-K selection over a specified number of rounds.

Symmetry-aware destruction. The most naive way to destroy a solution x is simply dropping $N_{destroy}$ of the last nodes from the sampled trajectory $\tau_{\rightarrow x}$. However, it only performs the destruc-

tion with one trajectory, while there can be multiple trajectories that correspond to the same solution x . Considering this symmetric nature, our destruction phase consists of 1) selecting $\tau'_{\rightarrow x}$ randomly from the set of symmetric trajectories and then 2) destroying τ'_x by dropping the last $N_{destroy}$ nodes, resulting in a partial solution. Note that the number of symmetric trajectories for a given solution differs from problem types, as discussed in Appendix E.

Reconstruction with temperature annealing. Given a partial solution, we reconstruct a new solution x' using the policy similar to the decoding steps explained in Section 4.2. Considering the purpose of the local search (refining a given solution), we further promote the exploitation by introducing an inverse temperature for the policy. Formally, we modify Equation (5) with the inverse temperature δ_r as follows:

$$P_F(s_{t+1}|s_t; \eta(\mathcal{G}; \theta), \rho, \delta_r) \propto \begin{cases} (\rho_{a_{t-1}, a_t} \eta_{a_{t-1}, a_t}(\mathcal{G}; \theta))^{\delta_r} & \text{if } a_t \notin s_t \\ 0 & \text{otherwise} \end{cases} \quad (15)$$

We increase δ_r linearly from 1.0 to a specified maximum value, δ_{\max} , as the local search round progresses.

Top-K selection. For a given solution x , we perform the aforementioned destruction and reconstruction multiple times (in batch), obtaining a set of refined solutions. Then we evaluate them and leave only top-K solutions among them in terms of solution quality. The remaining solutions are used as an initial solution for the next round of the search.

D Additional experiments

D.1 Comparison between trajectory balance and forward-looking detailed balance

We trained Attention Model (AM) [41] and heatmap-based policy from Joshi et al. [29] in an unsupervised way using FL-DB and TB loss. Table 6 shows the test results for 128 random TSP50 instances. The result is aligned with the previous observation from GFACS, showing the limitation of FL-DB loss for solving complex CO tasks.

Table 6: Comparison between forward-looking detailed balance (FL-DB) and trajectory balance (TB) loss in TSP50, using Attention Model (AM) and heatmap-based method from Joshi et al. [29] as backbone policies.

Method	TSP50	
	Obj.	Gap (%)
Concorde	5.69	0.00
AM + FL-DB (s.w. = 1280)	6.52	14.64
AM + TB (s.w. = 1280)	6.00	5.50
Joshi et al. + FL-DB (s.w. = 1280)	6.54	14.96
Joshi et al. + TB (s.w. = 1280)	6.09	7.05

D.2 Analysis of β and diversity-optimality trade-off

In this subsection, we explored the diversity-optimality trade-off by varying the inverse energy temperature β from low to high values. For analysis, we generate K solution samples from policies trained with GFACS with different values of β and DeepACO (with $\rho = 1$ so that the pheromone does not affect the result).

We use average pairwise Jaccard distance as a diversity metric. Formally, the diversity of a set of K solutions is calculated as $\frac{1}{K(K-1)} \sum_i \sum_j d_J(x_i, x_j)$, where d_J is a Jaccard distance between two solutions, defined as follows:

$$d_J(x_i, x_j) = 1 - J(x_i, x_j) = 1 - \frac{|E(x_i) \cap E(x_j)|}{|E(x_i) \cup E(x_j)|} \quad (16)$$

$E(x)$ is the set of edges composing the solution x . In TSP or CVRP, the (undirected) edge is a set of adjoining nodes in the solution path. For some CO problems, such as SMTWTP, the edge should be directed due to its asymmetric nature.

Figure 5 show that lower β values lead to more diverse solutions with higher costs, while higher β values result in less diverse solutions with lower costs. GFACS confirms the anticipated trade-off between diversity and optimality, establishing a Pareto frontier over DeepACO by offering more diverse and high-quality solutions. This advantage is particularly beneficial when an effective local search mechanism is available, increasing the likelihood of achieving superior local optima. However, excessively high β (e.g., 2000 in our result) degrades both diversity and solution quality, supposedly because too much high β hinders exploration during training. This empirical evidence supports our design choice of β annealing Appendix A.2, which encourages exploration in the early stage of training.

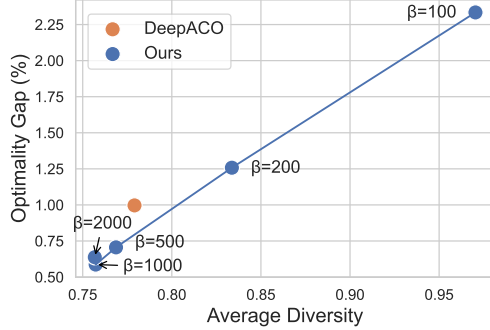


Figure 5: The trade-off between diversity and optimality as the inverse energy temperature β changes.

D.3 Evaluation with other ACO variants

Table 7: Evaluation results with different pheromone update rules, Elitist AS and MAX-MIN AS. We run $T = 10$ ACO rounds with 100 ants in all settings.

Method	TSP200		CVRP200	
	Obj.	Gap (%)	Obj.	Gap (%)
Concorde / PyVRP	10.72	0.00	27.93	0.00
AS	10.91	1.77	28.45	1.86
DeepACO + AS	10.77	0.45	28.44	1.80
GFACS + AS	10.75	0.26	28.32	1.40
Elitist AS	10.97	2.31	28.46	1.90
DeepACO + Elitist AS	10.77	0.49	28.45	1.84
GFACS + Elitist AS	10.75	0.28	28.34	1.47
MAX-MIN AS	10.97	2.34	28.46	1.88
DeepACO + MAX-MIN AS	10.78	0.57	28.44	1.82
GFACS + MAX-MIN AS	10.75	0.32	28.33	1.43

Our method is focused on enhancing the design of the heuristic matrix within the ACO framework. Thus, the advancement of the ACO algorithm itself (usually in pheromone update and action selection rule) is orthogonal to our work. To validate this claim, we evaluate our method with different ACO variants other than AS, namely Elitist Ant System [14], MAX-MIN Ant System [68]. The results in Table 7 demonstrate that GFACS consistently outperforms both ACO with human-designed heuristic and DeepACO under all pheromone update rules tested. This underscores the superiority of GFACS in generating a high-quality heuristic matrix.

D.4 Applying our method to other search algorithms

Table 8: Evaluation results combine with active search as posterior inference method.

Method	TSP200		CVRP200	
	Obj.	Gap (%)	Obj.	Gap (%)
Concorde / PyVRP	10.72	0.00	27.93	0.00
Pretrained GFACS				
– Off-policy TB Active Search	10.75	0.29	28.34	1.47
– On-policy RL Active Search	10.76	0.40	28.38	1.62
Pretrained DeepACO				
– On-policy RL Active Search	10.79	0.65	28.43	1.79

In this subsection, we study active search [3] rather than the pheromone update of ACO. In ACO, pheromone update is a posterior inference given a prior distribution (heuristic) for the probability model that generates the solutions. Similarly, we can think of active search as a posterior update that implicitly updates a given probability model by adjusting the parameters that generate it. We sample 20 solutions and take 5 gradient steps to update the parameter at each iteration. After 50 iterations, we report the average performance of the active search using our method with 3 seeds of 128 instances for each task. Table 8 shows that GAFCS integrates better with active search than DeepACO. This indicates that GAFCS is effective not only with heuristic-based posterior inference but also with learning-based posterior inference.

D.5 Comparison against TAM

Table 9: Results for CVRP instances used in TAM. The results for AM and TAM is drawn from Hou et al. [24], and the result for DeepACO is drawn from Ye et al. [79].

Method	CVRP100		CVRP400	
	Obj.	Time (s)	Obj.	Time (s)
AM*	16.42	0.06	29.33	0.20
TAM*	16.08	0.086	25.93	1.35
DeepACO ($T = 4$)	16.08	2.97	25.31	3.65
DeepACO ($T = 10$)	15.77	3.87	25.27	5.89
GFACS ($T = 4$)	15.77	1.07	24.95	3.23
GFACS ($T = 10$)	15.72	1.40	24.87	5.21

We compare GFACS and DeepACO against CVRP instances used in TAM [24]. These instances have a different capacity constraint from those we used for the main experiment (Table 1). Please refer to [24] for more details regarding the instance generation. Moreover, to match the processing time to be comparative to DeepACO, we set K (equal to the number of ants for ACO) to 16.

D.6 Ablation study

Table 10: Results of the ablation study. The mean and standard deviation are reported based on three independent runs. The reported gap is calculated against Concorde [2] for TSP and PyVRP [77] for CVRP.

Method	TSP500		CVRP500		BPP120
	Obj.	Gap (%)	Obj.	Gap (%)	Obj.
GFACS	16.0842 \pm 0.0043	1.56	64.1858 \pm 0.0071	1.95	51.8428 \pm 0.0706
– Off-policy Training	17.0861 \pm 0.0028	3.26	64.4248 \pm 0.0155	2.33	52.3158 \pm 0.1171
– Energy Reshaping	16.8718 \pm 0.0049	1.97	64.4121 \pm 0.0069	2.31	52.0654 \pm 0.0998
– Shared ϵ -norm	17.5209 \pm 0.0062	5.87	65.5069 \pm 0.0171	4.05	90.7332 \pm 9.1649
+ VarGrad [82]	16.8570 \pm 0.0086	1.88	64.2771 \pm 0.0293	2.09	51.9504 \pm 0.1222

In this section, we present the comprehensive results of our ablation study, incorporating standard deviations from multiple independent runs (three runs) to ensure statistical significance. The findings demonstrate that each component of our technical proposals contributes to improvement, supported by empirical and statistically rigorous evidence.

E Symmetric solutions of combinatorial optimization

This section delves into the symmetric characteristics of combinatorial solutions, wherein multiple trajectories, denoted as τ , can map to an identical combinatorial solution. We begin with a formal analysis focusing on two quintessential tasks: the Traveling Salesman Problem (TSP) and the Capacitated Vehicle Routing Problem (CVRP). This analysis lays the foundation for understanding the connections to other related combinatorial optimization problems.

Proposition E.1 (Symmetry Solution in TSP (Hamiltonian Cycle)). *Let $\mathcal{G} = (\mathcal{V}, \mathcal{D})$ be a finite, undirected graph where \mathcal{V} is the set of vertices and \mathcal{D} is the set of edges. Assume \mathcal{G} contains a Hamiltonian cycle. Denote $N = |\mathcal{V}|$ as the number of vertices. If $N > 1$, there exist exactly $2N$*

symmetric trajectories (including the cycle and its reverse) starting from each vertex in the cycle. For $N = 1$, there is exactly one identical trajectory.

Proof. A Hamiltonian cycle in \mathcal{G} is a cycle that visits every vertex exactly once. For $N > 1$, each cycle can be traversed in two distinct directions (clockwise and counterclockwise) from each vertex, yielding 2 trajectories per vertex. Since there are N vertices, this results in $2N$ symmetric trajectories. For $N = 1$, the cycle is trivial and only has one trajectory. \square

Proposition E.2 (Symmetric Solutions in CVRP). *Consider a Capacitated Vehicle Routing Problem (CVRP) defined on a graph $\mathcal{G} = (\mathcal{V}, \mathcal{D})$ with a designated depot vertex. Let there be K distinct Hamiltonian cycles (or routes) originating and terminating at the depot, and denote S as the number of single vertex cycles (excluding the depot) among these K cycles. The total number of symmetric solutions, considering the directionality of each cycle, is given by $K! \times 2^{K-S}$.*

Proof. Each of the K cycles can be ordered in $K!$ ways. Excluding the S single vertex cycles, each of the remaining $K - S$ cycles can be traversed in two directions (forward and reverse). Therefore, for these $K - S$ cycles, there are 2^{K-S} ways to choose a direction. The product $K! \times 2^{K-S}$ gives the total number of symmetric solutions for the CVRP under these conditions. \square

The propositions discussed previously can be extended to various variants of vehicle routing problems. Specifically, in the context of the orienteering problem (OP) and prize collecting traveling salesman problem (PCTSP), which represent special cases where $K = 1$, the number of symmetric trajectories is determined by the number of vertices, N , in the solution. When $N > 1$, there are exactly 2 symmetric trajectories for each route. In contrast, for a single-vertex solution ($N = 1$), the trajectory is identical, reflecting the singularity of the route.

F Extended related works

F.1 Deep constructive policy for neural combinatorial optimization

Constructive policy methods systematically build solutions by incrementally adding elements, beginning with an empty set and culminating in a complete solution. This approach ensures compliance with constraints by progressively narrowing the scope of actions, making it versatile for application in domains like vehicle routing [57, 41], graph combinatorial optimization [30, 1, 84], and scheduling [81].

In deep learning, various techniques adopt this constructive policy framework. Notably, the attention model (AM) [41] has been pivotal in vehicle routing problems (VRPs), establishing a new standard for stabilizing REINFORCE training. Subsequent advancements in AM have included enhanced decoder architecture [67, 78, 47], improved REINFORCE [76] baseline assessments [43, 37], leveraging symmetries for sample efficiency [32], the application of population-based reinforcement learning (RL) [21], ensemble-based learning [27, 86] and refined solution-building methods [16]. Recent advancements in hierarchical algorithms exploit AM-based policies for solution optimization: one policy broadly generates solutions while another refines them locally [36, 24, 80]. Additionally, AM-driven constructive policies have been effectively applied in hardware routing [34, 35] and placement tasks [60, 31].

Graph combinatorial optimization, particularly in problems like maximum independent sets, has diversified from contrived VRPs policies due to their local decomposability and the relative ease of training value functions for partial solutions where VRPs are not locally decomposable due to their global contains. Starting with the influential works by Khalil et al. [30], which employed deep Q networks [55] for graph policy training, creating solutions constructively, Ahn et al. [1] introduced an innovative Markov Decision Process (MDP) to generate multiple solution components per iteration by exploiting the local decomposability of graph combinatorial problems. Zhang et al. [84] further developed this concept, training their MDP with forward-looking GFlowNets [59].

Our research aligns with the deep constructive policy framework, where GFlowNets constructively build actions from an initial empty solution (s_0) to a final complete solution (s_n). Additionally, our methods include a heatmap-based approach, detailed in [Appendix F.3](#).

F.2 Deep improvement policy for neural combinatorial optimization

The improvement policy focuses on refining complete solutions, similar to local search methods like 2opt [11]. Its advantage lies in achieving comparable performances to constructive policies, especially when allotted sufficient time for extensive improvement iterations. Researchers typically adapt existing heuristic local search techniques, creating learning policies that emulate these methods through maximizing expected returns via reinforcement learning [12, 22, 48–50, 33]. Also, recent works have explored active search to refine solutions via policy adjustments [23, 66] or sampling the conditions from a continuous latent space [7]. Moreover, alternative strategies using discrete Langevin sampling instead of neural networks have shown promising outcomes [69]. This approach serves as a complementary extension to deep constructive policies, as it often enhances solutions initially formulated by constructive methods. Additionally, our method, which integrates local search into the training loop, could see further enhancements if advancements in this area are incorporated into our training procedures.

F.3 Heatmap-based neural combinatorial optimization

The heatmap-based method [29] entails the acquisition of a graph representation, referred to as the "Heatmap," from input graph instances. This Heatmap serves as a prior distribution, influencing the generation of a solution. However, this approach is not self-contained and requires an additional solution construction step, which may involve techniques like beam search [29], dynamic programming [42], Monte Carlo tree search [20, 62, 70] or greedy search with a guide using an objective function [44]. The key advantage of the heatmap-based method lies in its exceptional generalizability when compared to constructive policies. It operates at an abstract level, free from the constraints inherent in generating actual combinatorial solutions.

Our approach falls under heatmap-based methodologies, where we learn a heuristic metric (i.e., heatmap) and employ ant colony optimization for solution construction. A key advantage of our method over many other supervised learning-based heatmap approaches is its independence from optimally labeled data.

Broader Impact

We proposed a new probabilistic approach that can be trained using off-policy learning and applied to various combinatorial optimization problems, such as vehicle routing and scheduling. This method is relevant to industrial engineering, particularly in optimizing transportation and manufacturing processes, and can potentially extend to scientific discovery through chemical structure and biological sequence optimization. It is important to consider the ethical implications of probabilistic optimization methods, as they carry the potential for misuse in fields such as harmful drug discovery. While these algorithms offer several benefits, their application should be carefully monitored to ensure responsible and ethical use, minimizing the risk of unintended negative consequences.